

1 **Environmental responses, not species interactions, determine synchrony of**
2 **dominant species in semiarid grasslands**

3 Andrew T. Tredennick¹, Claire de Mazancourt², Michel Loreau², and Peter B. Adler¹

4 *¹Department of Wildland Resources and the Ecology Center, 5230 Old Main Hill, Utah State University,*
5 *Logan, Utah 84322 USA*

6 *²Centre for Biodiversity Theory and Modelling, Theoretical and Experimental Ecology Station, CNRS and*
7 *Paul Sabatier University, Moulis, 09200, France*

8 **Running Head:** Drivers of species synchrony in grasslands

9 **Corresponding Author:**

10 Andrew Tredennick
11 Department of Wildland Resources and the Ecology Center
12 Utah State University
13 5230 Old Main Hill
14 Logan, Utah 84322 USA
15 Phone: +1-970-443-1599
16 Fax: +1-435-797-3796
17 Email: atredenn@gmail.com

Abstract

19 Temporal asynchrony among species helps diversity to stabilize ecosystem functioning,
 20 but identifying the mechanisms that determine synchrony remains a challenge. Here, we
 21 refine and test theory showing that synchrony depends on three factors: species responses to
 22 environmental variation, interspecific interactions, and demographic stochasticity. We then
 23 conduct simulation experiments with empirical population models to quantify the relative
 24 influence of these factors on the synchrony of dominant species in five semiarid grasslands.
 25 We found that the average synchrony of per capita growth rates, which can range from 0
 26 (perfect asynchrony) to 1 (perfect synchrony), was higher when environmental variation
 27 was present (0.62) rather than absent (0.43). Removing interspecific interactions and demo-
 28 graphic stochasticity had small effects on synchrony. For the dominant species in these plant
 29 communities, where species interactions and demographic stochasticity have little influence,
 30 synchrony reflects the covariance in species responses to the environment.

31 *Key words:* synchrony, compensatory dynamics, environmental stochasticity, demo-
 32 graphic stochasticity, interspecific competition, stability, grassland

INTRODUCTION

34 Ecosystems are being transformed by species extinctions (Cardinale et al. 2012), changes in com-
 35 munity composition (Vellend et al. 2013, Dornelas et al. 2014), and anthropogenic environmental
 36 change (Vitousek et al. 1997), impacting the provisioning and stability of ecosystem services
 37 (Loreau et al. 2001, Hooper et al. 2005, Rockstrom et al. 2009). Experiments have provided com-
 38 pelling evidence that decreases in species richness will decrease productivity (Tilman et al. 2001)
 39 and the temporal stability of productivity (Tilman et al. 2006, Hector et al. 2010). The stabilizing
 40 effect of species richness arises from a combination of selection effects and complementarity
 41 (Loreau and Hector 2001). Selection effects occur when a dominant species has higher than av-
 42 erage temporal variability, which generates a negative effect on ecosystem stability (e.g., Grman

43 et al. 2010). Complementarity occurs when species have unique dynamics through time, causing
44 their abundances to fluctuate asynchronously. All else being equal, lower synchrony of species
45 dynamics through time results in greater ecosystem stability (Loreau and de Mazancourt 2013).
46 The link between synchrony and stability means that a mechanistic understanding of synchrony
47 can help us predict the impacts of global change on ecosystem stability.

48 Asynchronous dynamics, also known as compensatory dynamics (Gonzalez and Loreau
49 2009), result from individual species responding in different ways to environmental fluctuations,
50 random chance events, and/or competitive interactions (Isbell et al. 2009, Hector et al. 2010,
51 de Mazancourt et al. 2013, Gross et al. 2014). Species richness affects the degree of synchrony
52 in a community because larger species pools are more likely to contain species that respond
53 dissimilarly to environmental conditions, reducing synchrony (Yachi and Loreau 1999). More
54 species rich communities may also exhibit lower synchrony, and thus higher stability, due to a
55 greater chance of strong species interactions (Gross et al. 2014). Determining whether synchrony
56 is primarily an outcome of species-specific responses to environmental conditions or interspe-
57 cific competition is thus an important step toward understanding how species losses and abiotic
58 changes will impact ecosystem stability (Hautier et al. 2014).

59 Theory identifies three main determinants of species synchrony: environmental stochastic-
60 ity, demographic stochasticity, and interspecific interactions (Loreau and de Mazancourt 2008,
61 2013, Gonzalez and Loreau 2009). For example, in a community composed of large populations
62 (no demographic stochasticity) with weak interspecific interactions, community-wide species
63 synchrony should be determined by the covariance of species' responses to the environment
64 (Loreau and de Mazancourt 2008). However, this prediction relies on a relatively simple popu-
65 lation model and only holds under two assumptions: (i) species' responses to the environment
66 are similar in magnitude and (ii) all species have similar growth rates. Whether such theoretical
67 predictions hold in natural communities where species differences are unlikely to be symmetrical
68 is unknown because few studies have explicitly tested theory on the drivers of species synchrony
69 in natural communities (Mutshinda et al. 2009, Thibaut et al. 2012), and they did not consider

70 demographic stochasticity.

71 In grasslands, most empirical studies have focused on whether species synchrony is primar-
72 ily an outcome of species-specific responses to environmental conditions (Hautier et al. 2014)
73 or competition (Gross et al. 2014). Even beyond grassland studies, whether competition or envi-
74 ronmental responses drive compensatory dynamics remains controversial (reviewed in Gonzalez
75 and Loreau 2009). In part, controversy remains because quantifying the relative strengths of
76 each driver on the degree of synchrony from the covariance matrix of species abundances (e.g.,
77 Houlahan et al. 2007) is impossible. This is because an unbiased null expectation for synchrony
78 does not exist (Loreau and de Mazancourt 2008) and observed synchrony can arise from non-
79 unique combinations of factors (Ranta et al. 2008). For example, weak synchrony of population
80 abundances could reflect positive environmental correlations (synchronizing effect) offset by
81 strong competition (desynchronizing effect), or negative environmental correlations and weak
82 competition.

83 The best way to quantify the effects of environmental stochasticity, demographic stochastic-
84 ity, and interspecific interactions is to remove them one-by-one, and in combination. In principle,
85 this could be done in an extremely controlled laboratory setting (e.g., Venail et al. 2013), but
86 empirically-based models of interacting populations, fit with data sets from natural communities,
87 offer a practical alternative. For example, Mutshinda et al. (2009) fit a dynamic population model
88 to several community time series of insect and bird abundances. They used a statistical technique
89 to decompose temporal variation into competition and environmental components, and found
90 that positively correlated environmental responses among species determined community dynam-
91 ics. Thibaut et al. (2012) used a similar approach for reef fish and came to a similar conclusion:
92 environmental responses determine synchrony.

93 While a major step forward, Mutshinda et al.'s (2009) and Thibaut et al.'s (2012) modeling
94 technique does have some limitations. First, although both studies quantified the relative impor-
95 tance of environmental stochasticity and interspecific interactions to explain the observed vari-

96 action of species synchrony, they did not use the model to quantify how much synchrony would
97 change if each factor were removed. Second, they relied on abundance data that may or may not
98 reliably capture competitive interactions that occur at the individual level. Third, fluctuations in
99 abundance may mask the mechanisms that underpin species synchrony [@Loreau2008a] and
100 ecosystem stability (Loreau and de Mazancourt 2013) due to legacy effects and ecological drift.
101 Theory indicates that a focus on the fluctuations of species' per capita growth rates better reveals
102 the mechanisms that ultimately determine species synchrony (Loreau and de Mazancourt 2008),
103 which is why we focus on per capita growth rates.

104 Here, we use multi-species population models fit to long-term demographic data from five
105 semi-arid plant communities to test theory on the drivers of species synchrony (Fig. 1). Our
106 objectives are to (1) derive and test theoretical predictions of species synchrony and (2) determine
107 the relative influence of environmental stochasticity, demographic stochasticity, and interspecific
108 interactions on **the synchrony of dominant species** in natural plant communities. Our focus is
109 limited to dominant species due to data constraints, but previous work indicates that the dynamics
110 of dominant species are most important for ecosystem functioning in grasslands (Smith and
111 Knapp 2003, Bai et al. 2004, Grman et al. 2010, Sasaki and Lauenroth 2011).

112 To achieve our objectives, we first refine theory that has been used to predict the effects
113 of species richness on ecosystem stability (de Mazancourt et al. 2013) and species synchrony
114 (Loreau and de Mazancourt 2008) to generate predictions of community-wide species synchrony
115 under two limiting cases derived from the dynamics of individual species in monoculture. We
116 then confront our theoretical predictions with simulations from the empirically-based population
117 models. Second, we use the multi-species population models to perform simulation experiments
118 that isolate the effects of environmental stochasticity, demographic stochasticity, and interspecific
119 interactions on community-wide species synchrony. Given that our population models capture
120 the essential features of community dynamics important to synchrony (density-dependence, and
121 demographic and environmental stochasticity), and that these models successfully reproduce
122 observed community dynamics (Chu and Adler 2015), perturbing the models can reveal the

123 processes that determine synchrony of dominant species in our focal grassland communities.

124

THEORETICAL MODEL

125 **The model**

126 While existing theory has identified environmental responses, demographic stochasticity, and
127 species interactions as the drivers of the temporal synchrony of species' per capita growth rates,
128 and thus abundances, we do not have a simple expression to predict synchrony in a particular
129 community with all factors operating simultaneously. However, we can derive analytical predic-
130 tions for species synchrony under special limiting cases. The limiting case predictions we derive
131 serve as baselines to help us interpret results from empirically-based simulations (described be-
132 low). We focus on synchrony of per capita growth rates, rather than abundances, because growth
133 rates represent the instantaneous response of species to the environment and competition, and are
134 less susceptible to the legacy effects of drift and disturbance (Loreau and de Mazancourt 2008).
135 We present equivalent results for synchrony of species abundances in the Appendix S1, and show
136 that they lead to the same overall conclusions as synchrony of per capita growth rates.

137 Following Loreau and de Mazancourt (2008) and de Mazancourt et al. (2013), we define
138 population growth, ignoring observation error, as

$$r_i(t) = \ln N_i(t+1) - \ln N_i(t) \quad (1)$$

$$= r_{mi} \left[1 - \frac{N_i(t) + \sum_{j \neq i} \alpha_{ij} N_j(t)}{K_i} + \sigma_{ei} u_{ei}(t) + \frac{\sigma_{di} u_{di}(t)}{\sqrt{N_i(t)}} \right] \quad (2)$$

139 where $N_i(t)$ is the biomass of species i in year t , and $r_i(t)$ is its population growth rate in year t .
140 r_{mi} is species i 's intrinsic rate of increase, K_i is its carrying capacity, and α_{ij} is the interspecific
141 competition coefficient representing the effect of species j on species i . Environmental stochas-

142 ticity is incorporated as $\sigma_{ei} u_{ei}(t)$, where σ_{ei}^2 is the temporal variance of environmental conditions.
 143 Species-specific environmental responses are included as u_{ei} , which are normal random vari-
 144 ables with zero mean and unit variance that are independent through time but may be correlated
 145 between species. Demographic stochasticity arises from variations in births and deaths among
 146 individuals (e.g., same states, different fates), and is included in the model as a first-order, normal
 147 approximation (Lande et al. 2003, de Mazancourt et al. 2013). σ_{di}^2 is the demographic variance
 148 (i.e., the intrinsic demographic stochasticity of species i) and $u_{di}(t)$ are independent normal vari-
 149 ables with zero mean and unit variance that allow demographic stochasticity to vary through
 150 time.

151 To derive analytical predictions we solved a first-order approximation of Equation 2 (de
 152 Mazancourt et al. 2013 and Appendix S1). Due to the linear approximation approach, our analyti-
 153 cal predictions will likely fail in communities where species exhibit large fluctuations due to limit
 154 cycles and chaos (Loreau and de Mazancourt 2008). Indeed, one of the advantages of focusing
 155 on growth rates rather than abundances is that growth rates are more likely to be well-regulated
 156 around an equilibrium value, if the long-term average of a species' growth rate is relatively small
 157 (e.g., $r < 2$).

158 Predictions

159 Our first prediction assumes no interspecific interactions, no environmental stochasticity, iden-
 160 tical intrinsic growth rates, and that demographic stochasticity is operating but all species have
 161 identical demographic variances. This limiting case, \mathcal{M}_D , represents a community where dynam-
 162 ics are driven by demographic stochasticity alone. Our prediction for the synchrony of per capita
 163 growth rates for \mathcal{M}_D , ϕ_{R,\mathcal{M}_D} , is

$$\phi_{R,\mathcal{M}_D} = \frac{\sum_i p_i^{-1}}{\left(\sum_i p_i^{-1/2}\right)^2}, \quad (3)$$

164 where p_i is the average frequency of species i , $p_i = N_i/N_T$. When all species have identical
165 abundances and $p_i = 1/S$, where S is species richness, synchrony equal $1/S$ (Loreau and de
166 Mazancourt 2008).

167 Our second limiting case assumes only environmental stochasticity is operating (\mathcal{M}_E).
168 Thus, we assume there are no interspecific interactions, demographic stochasticity is absent,
169 intrinsic growth rates are identical, and environmental variance is identical for all species. Our
170 prediction for the synchrony of per capita growth rates for \mathcal{M}_E , ϕ_{R,\mathcal{M}_E} , is

$$\phi_{R,\mathcal{M}_E} = \frac{\sum_{i,j} \text{cov}(u_{ei}, u_{ej})}{S^2}, \quad (4)$$

171 where $\text{cov}(u_{ei}, u_{ej})$ is the standardized covariance of environmental responses between species i
172 and species j .

173 Confronting our theoretical predictions with data requires estimates of species dynamics of
174 large populations (no demographic stochasticity) growing in isolation (no interspecific interac-
175 tions) to calculate the covariance of species' environmental responses. To estimate environmental
176 responses in natural communities, we turn to our population models built using long-term demo-
177 graphic data.

178 EMPIRICAL ANALYSIS

179 Materials and methods

180 **Data** We use long-term demographic data from five semiarid grasslands in the western United
181 States (described in detail by Chu and Adler 2015). Each site includes a set of 1-m² permanent
182 quadrats within which all individual plants were identified and mapped annually using a panto-
183 graph (Hill 1920). The resulting mapped polygons represent basal cover for grasses and canopy
184 cover for shrubs. Data come from the Sonoran desert in Arizona (Anderson et al. 2012), sage-

brush steppe in Idaho (Zachmann et al. 2010), southern mixed prairie in Kansas (Adler et al. 2007), northern mixed prairie in Montana (Anderson et al. 2011), and Chihuahuan desert in New Mexico (Anderson et al. in preparation, Chu and Adler 2015) (Table 1).

Calculating observed synchrony The data consist of records for individual plant size in quadrats for each year. To obtain estimates of percent cover for each focal species in each year, we summed the individual-level data within quadrats and then averaged percent cover, by species, over all quadrats. We calculated per capita growth rates as $\log(x_t) - \log(x_{t-1})$, where x is species' percent cover in year t . Using the community time series of per capita growth rates or percent cover, we calculated community synchrony using the metric of Loreau and de Mazancourt (2008) in the ‘synchrony’ package (Gouhier and Guichard 2014) in R (R Core Team 2013). Specifically, we calculated synchrony as

$$\phi_r = \frac{\sigma_T^2}{(\sum_i \sigma_{r_i})^2} \quad (5)$$

where σ_{r_i} is the temporal standard deviation of species i 's per capita population growth rate (r_i) and σ_T^2 is the temporal variance of the aggregate community-level growth rate. ϕ ranges from 0 at perfect asynchrony to 1 at perfect synchrony (Loreau and de Mazancourt 2008). We use the same equation to calculate observed synchrony of species' percent cover, which we present to relate our results to previous findings, even though we focus on synchrony of growth rates in our model simulations (see below).

Fitting statistical models Vital rate regressions are the building blocks of our dynamic models: an integral projection model (IPM) and an individual-based model (IBM). We followed the approach of Chu and Adler (2015) to fit statistical models for survival, growth, and recruitment (see Appendix S1 for full details). We modeled survival probability of each genet as function of genet size, temporal variation among years, permanent spatial variation among groups of quadrats, and local neighborhood crowding from conspecific and heterospecific genets. Regression coefficients

208 for the effect of crowding by each species can be considered a matrix of interaction coefficients
209 whose diagonals represent intraspecific interactions and whose off-diagonals represent interspe-
210 cific interactions (Adler et al. 2010). These interaction coefficients can take positive (facilitative)
211 or negative (competitive) values. We modeled growth as the change in size of a genet from one
212 year to the next, which depends on the same factors as the survival model. We fit the survival
213 and growth regressions using INLA (Rue et al. 2014), a statistical package for fitting generalized
214 linear mixed effects models via approximate Bayesian inference (Rue et al. 2009), in R (R Core
215 Team 2013). Spatial (quadrat groupings) variation was treated as a random effect on the intercept
216 and temporal (interannual) variation was treated as random effects on the intercept and the effect
217 of genet size in the previous year (Appendix S1).

218 Interspecific and intraspecific crowding, which represent species interactions, can be in-
219 cluded as fixed effects or as random effects that vary each year. In the latter case, important
220 yearly crowding effects would indicate an interaction between environmental conditions and
221 species interactions because we assume that the yearly random effects encompass environmental
222 variability, generally. We tested for environment-species interactions by comparing models with
223 and without yearly random effects on crowding. In the end, crowding was treated as a fixed effect
224 without a temporal component because most 95% credible intervals for random year effects on
225 crowding broadly overlapped zero and, in a test case, including yearly crowding effects did not
226 change our results.

227 We modeled recruitment at the quadrat scale, rather than the individual scale, because the
228 original data do not attribute new genets to specific parents (Chu and Adler 2015). Our recruit-
229 ment model assumes that the number of recruits produced in each year follows a negative bino-
230 mial distribution with the mean dependent on the cover of the parent species, permanent spatial
231 variation among groups, temporal variation among years, and inter- and intraspecific interac-
232 tions as a function of total species' cover in the quadrat. We fit the recruitment model using a
233 hierarchical Bayesian approach implemented in JAGS (Plummer 2003) using the 'rjags' package
234 (Plummer 2014) in R (R Core Team 2013). Again, temporal and spatial variation were treated as

235 random effects.

236 **Building dynamic multi-species models** Once we have fit the vital rate statistical models,
237 building the population models is straightforward. For the IBM, we initialize the model by
238 randomly assigning plants spatial coordinates, sizes, and species identities until each species
239 achieves a density representative of that observed in the data. We then project the model forward
240 by using the survival regression to determine whether a genet lives or dies, the growth regression
241 to calculate changes in genet size, and the recruitment regression to add new individuals that are
242 distributed randomly in space. Crowding is directly calculated at each time step since each genet
243 is spatially referenced. Environmental stochasticity is not an inherent feature of IBMs, but is
244 easily included since we fit year-specific temporal random effects for each vital rate regression.
245 To include temporal environmental variation, at each time step we randomly choose a set of es-
246 timated survival, growth, and recruitment parameters specific to one observation year. For all
247 simulations, we ignore the spatial random effect associated with variation among quadrat groups,
248 so our simulations represent an average quadrat for each site.

249 The IPM uses the same vital rate regressions as the IBM, but it is spatially implicit and does
250 not include demographic stochasticity. Following Chu and Adler (2015), we use a mean field ap-
251 proximation that captures the essential features of spatial patterning to define the crowding index
252 at each time step (Supporting Online Information). Temporal variation is included in exactly the
253 same way as for the IBM. For full details on the IPMs we use, see Chu and Adler (2015).

254 **Simulation experiments** We performed simulation experiments where drivers (environmental
255 stochasticity, demographic stochasticity, or interspecific interactions) were removed one-by-
256 one and in combination. To remove interspecific interactions, we set the off-diagonals of the
257 interaction matrix for each vital rate regression to zero. This retains intraspecific interactions,
258 and thus density-dependence, and results in simulations where species are growing in isolation.
259 We cannot definitively rule out the effects of species interactions on all parameters, meaning

260 that a true monoculture could behave differently than our simulations of a population growing
261 without interspecific competitors. To remove the effect of a fluctuating environment, we removed
262 the temporal (interannual) random effects from the regression equations. To remove the effect
263 of demographic stochasticity, we use the IPM rather than the IBM because the IPM does not
264 include demographic stochasticity (demographic stochasticity cannot be removed from the IBM).
265 Since the effect of demographic stochasticity on population dynamics depends on population
266 size (Lande et al. 2003), we can control the strength of demographic stochasticity by simulating
267 the IBM on areas (e.g. plots) of different size. Results from an IBM with infinite population size
268 would converge on results from the IPM. Given computational constraints, the largest landscape
269 we simulate is a 25 m² plot.

270 We conducted the following six simulation experiments: (1) IBM: All drivers (environmental
271 stochasticity, demographic stochasticity, or interspecific interactions) present; (2) IPM:
272 Demographic stochasticity removed; (3) IBM: Environmental stochasticity removed; (4) IBM: In-
273 terspecific interactions removed; (5) IPM: Interspecific interactions and demographic stochastic-
274 ity removed; (6) IBM: Interspecific interactions and environmental stochasticity removed. We do
275 not include a simulation with only interspecific interactions because our population models run to
276 deterministic equilibriums in the absence of environmental or demographic perturbations. We ran
277 IPM simulations for 2,000 time steps, after an initial 500 iteration burn-in period. This allowed
278 species to reach their stable size distribution. We then calculated yearly per capita growth rates
279 from the simulated time series, and then calculated the synchrony of species' per capita growth
280 rates over 100 randomly selected contiguous 50 time-step sections.

281 We ran IBM simulations for 100 time steps, and repeated the simulations 100 times for each
282 simulation experiment. From those, we retained only the simulations in which no species went
283 extinct due to demographic stochasticity. Synchrony of per capita growth rates was calculated
284 over the 100 time steps for each no extinction run within a model experiment. In the IBM sim-
285 ulations the strength of demographic stochasticity should weaken as population size increases,
286 meaning that synchrony should be less influenced by demographic stochasticity in large popu-

287 lations compared to small populations. To explore this effect, we ran simulations (4) and (6) on
288 plot sizes of 1, 4, 9, 16, and 25 m². All other IBM simulations were run on a 25 m² landscape to
289 most closely match the implicit spatial scale of the IPM simulations.

290 Our simulations allow us to quantify the relative importance of environmental responses,
291 species interactions, and demographic stochasticity by comparing the simulation-based values of
292 community-wide species synchrony. Results from our simulation experiments also allow us to
293 test our theoretical predictions. First, in the absence of interspecific interactions and demographic
294 stochasticity, populations can only fluctuate in response to the environment. Therefore, we can
295 use results from simulation (5) to estimate the covariance of species' responses to the environ-
296 ment ($\text{cov}(u_{ie}, u_{je})$) and parameterize Equation 4. Parameterizing Equation 3 does not require
297 simulation output because the only parameters are the species' relative abundances. Second, sim-
298 ulations (5) and (6) represent the simulated version of our limiting case theoretical predictions.
299 Thus, we directly test the theoretical predictions by comparing them to observed synchrony and
300 simulated synchrony.

301 Results

302 Observed synchrony of species' per capita growth rates at our study sites range from 0.36 to
303 0.89 and synchrony of percent cover ranged from 0.15 to 0.92 (Table 2). Synchrony of per capita
304 growth rates and CV of percent cover are positively correlated (Pearson's $\rho = 0.72, N = 5$). For
305 all five communities, species synchrony from IPM and IBM simulations closely approximated
306 observed synchrony (Fig. S1). IBM-simulated synchrony is consistently, but only slightly, lower
307 than IPM-simulated synchrony (Fig. S1), likely due to the desynchronizing effect of demographic
308 stochasticity.

309 Across the five communities, our limiting case predictions closely matched synchrony from
310 the corresponding simulation experiment (Fig. 2 and Table S1). The correlation between our
311 analytical predictions and simulated synchrony was 0.97 for ϕ_{R,\mathcal{M}_D} ($N = 5$) and 0.997 for ϕ_{R,\mathcal{M}_E}

312 ($N = 5$). The largest difference between predicted and simulated synchrony was 0.05 in New
313 Mexico for ϕ_{R,\mathcal{M}_D} (Table S1).

314 Simulation experiments revealed that removing environmental fluctuations has the largest
315 impact on synchrony, leading to a reduction in synchrony of species growth rates in four out
316 of five communities (Fig. 2). Removing environmental fluctuations (“No E.S.” simulations) de-
317 creased synchrony by 33% in Arizona, 48% in Kansas, 39% in Montana, and 40% in New Mex-
318 ico. Only in Idaho did removing environmental fluctuations cause an increase in synchrony (Fig.
319 2), but the effect was small (9% increase; Table S2). Overall, species’ temporal random effects
320 in the statistical vital rate models are positively, but not perfectly, correlated (Table S3). Our ap-
321 proach assumes that these temporal random effects represent environmental responses, meaning
322 that positively correlated temporal random effects indicate positively correlated environmental
323 responses.

324 Species interactions are weak in these communities (Table S4 and Chu and Adler 2015),
325 and removing interspecific interactions had little effect on synchrony (Fig. 2; “No Comp.” simu-
326 lations). Removing interspecific interactions caused, at most, a 5% change in synchrony (Fig. 2
327 and Table S2). Removing demographic stochasticity (“No D.S.” simulations) caused synchrony
328 to increase slightly in all communities (Fig. 2), with an average 6% increase over synchrony from
329 IBM simulations on a 25m² area.

330 In IBM simulations, the desynchronizing effect of demographic stochasticity, which in-
331 creases as population size decreases, modestly counteracted the synchronizing force of the en-
332 vironment, but not enough to lower synchrony to the level observed when only demographic
333 stochasticity is operating (Fig. 3). In the largest, 25 m² plots, synchrony was driven by environ-
334 mental stochasticity (e.g., \mathcal{M}_E). At 1 m², synchrony reflected the combined effects of demo-
335 graphic stochasticity and environmental stochasticity (e.g., simulated synchrony fell between
336 \mathcal{M}_E and \mathcal{M}_D). For context, population sizes increased from an average of 17 individuals per
337 community in 1 m² IBM simulations to an average of 357 individuals per community in 25 m²

338 IBM simulations.

339 Results for synchrony of percent cover are qualitatively similar, but simulation results were
340 more variable and less consistent with analytical predictions and observed synchrony (Appendix
341 S1, Figs. S2-S3).

342 DISCUSSION

343 Our study produced four main findings that were generally consistent across five natural plant
344 communities: (1) limiting-case predictions from the theoretical model were well-supported by
345 simulations from the empirical models; (2) demographic stochasticity decreased community syn-
346 chrony, as expected by theory, and its effect was largest in small populations; (3) environmental
347 fluctuations increased community synchrony relative to simulations in constant environments
348 because species-specific responses to the environment were positively, though not perfectly, corre-
349 lated; and (4) interspecific interactions were weak and therefore had little impact on community
350 synchrony. We also found that analyses based on synchrony of species' percent cover, rather than
351 growth rates, were uninformative (Figs. S2-S3) since the linear approximation required for an-
352 alytical predictions is a stronger assumption for abundance than growth rates, especially given
353 relatively short time-series (Appendix S1). Thus, our results provide further evidence that it is
354 difficult to decipher mechanisms of species synchrony from abundance time series, as expected
355 by theory (Loreau and de Mazancourt 2008). Observed synchrony of per capita growth rates was
356 positively correlated with the variability of percent cover across our focal communities, which
357 confirms that we are investigating an important process underlying ecosystem stability.

358 Simulations support theoretical predictions

359 Our theoretical predictions were derived from a simple model of population dynamics and re-
360 quired several simplifying assumptions, raising questions about their relevance to natural com-
361 munities. For example, the species in our communities do not have equivalent environmental and

362 demographic variances (Figs. S4-S7), as required by our predictions. However, the theoretical
363 predictions closely matched results from simulations of population models fit to long-term data
364 from natural plant communities (Table S1). Strong agreement between our analytical predictions
365 and the simulation results should inspire confidence in the ability of simple models to inform
366 our understanding of species synchrony even in complex natural communities, and allows us to
367 place our simulation results within the context of contemporary theory. **However, whether the**
368 **theoretical model adequately represents more complex communities remains unknown because**
369 **we had to focus on dominant species.**

370 **Demographic stochasticity decreases synchrony in small populations**

371 In large populations, removing demographic stochasticity had no effect on species synchrony
372 (Fig. 2). In small populations, demographic stochasticity partially counteracted the synchronizing
373 effects of environmental fluctuations and interspecific interactions on per capita growth rates, in
374 agreement with theory (Loreau and de Mazancourt 2008). **This is shown in Fig. 3, where IBM**
375 **simulations with environmental forcing and demographic stochasticity have higher synchrony**
376 **than simulations with only demographic stochasticity, but the differences between simulations**
377 **are smaller at lower population sizes.** Even in small populations (e.g., 1 m² landscapes), however,
378 demographic stochasticity was not strong enough to compensate the synchronizing effects of
379 environmental fluctuations and match the analytical prediction where only demographic stochas-
380 ticity is operating (\mathcal{M}_D in Fig. 3). These results confirm the theoretical argument by Loreau and
381 de Mazancourt (2008) that independent fluctuations among interacting species in a non-constant
382 environment should be rare. Only in the Idaho community does synchrony of per capita growth
383 rates approach \mathcal{M}_D in a non-constant environment (Fig. 3). This is most likely due to the strong
384 effect of demographic stochasticity on the shrub *Artemisia tripartita* since even a 25 m² quadrat
385 would only contain a few individuals of that species.

386 Our analysis of how demographic stochasticity affects synchrony demonstrates that syn-

387 chrony depends on the observation area. As the observation area increases, population size in-
388 creases and the desynchronizing effect of demographic stochasticity lessens (Fig. 3). Thus, our
389 results suggest that community-wide species synchrony will increase as the observation area
390 increases, rising from \mathcal{M}_D to \mathcal{M}_E . Such a conclusion assumes, however, that species richness re-
391 mains constant as observation area increases, which is unlikely (Taylor 1961). Recent theoretical
392 work has begun to explore the linkage between ecosystem stability and spatial scale (Wang and
393 Loreau 2014, 2016), and our results suggest that including demographic stochasticity in theoreti-
394 cal models of metacommunity dynamics may be important for understanding the role of species
395 synchrony in determining ecosystem stability across spatial scales.

396 **Environmental fluctuations drive community synchrony**

397 In large populations where interspecific interactions are weak, synchrony is expected to be driven
398 exclusively by environmental fluctuations (Equation 4). Under such conditions community syn-
399 chrony should approximately equal the synchrony of species' responses to the environment
400 (Loreau and de Mazancourt 2008). Two lines of evidence lead us to conclude that environmen-
401 tal fluctuations drive species synchrony in our focal plant communities. First, in our simulation
402 experiments, removing interspecific interactions resulted in no discernible change in community-
403 wide species synchrony of per capita growth rates (Fig. 2). Second, removing environmental
404 fluctuations from simulations consistently reduced synchrony (Fig. 2). Our results lead us to
405 conclude that environmental fluctuations, not species interactions, are the primary driver of
406 community-wide species synchrony [among the dominant species](#) we studied. Given accumu-
407 lating evidence that niche differences in natural communities are large (reviewed in Chu and
408 Adler 2015), and thus species interactions are likely to be weak, our results may be general in
409 natural plant communities.

410 In the Idaho community, removing environmental fluctuations did not cause a large de-
411 crease in synchrony. However, that result appears to be an artifact. Removing environmental

412 variation results in a negative invasion growth rate for *A. tripartita*. Although we only analyzed
413 IBM runs in which *A. tripartita* had not yet gone extinct, it was at much lower abundance than
414 in the other simulation runs. When we removed *A. tripartita* from all simulations, the Idaho re-
415 sults conformed with results from all other sites: removing environmental stochasticity caused
416 a significant reduction in species synchrony (Fig. S8). Our main results for Idaho (Fig. 2), with
417 *A. tripartita* included, demonstrate how the processes that determine species synchrony interact
418 in complex ways. *A. tripartita* has a facilitative effect on each grass species across all vital rates,
419 except for a small competitive effect on *H. comata*'s survival probability (Tables S8-S10). At the
420 same time, all the perennial grasses have negative effects on each other for each vital rate (Tables
421 S8-S10). We know synchrony is affected by interspecific competition (Loreau and de Mazancourt
422 2008), but how facilitative effects manifest themselves is unknown. The interaction of facilita-
423 tion and competition is clearly capable of having a large effect on species synchrony, and future
424 theoretical efforts should aim to include a wider range of species interactions.

425 Environmental responses synchronized dynamics relative to a null expectation of inde-
426 pendent species interactions (e.g., "No Comp. + No E.S." simulations in Fig. 2), but observed
427 and simulated synchrony was still less than one in all cases (Fig. 2). Asynchronous dynam-
428 ics result because the responses of these species to environmental conditions are sufficiently
429 different. Many studies of ecosystem stability in semiarid grasslands focus on tradeoffs among
430 dominant functional types, such as grasses versus forbs (Sasaki and Lauenroth 2011) or among
431 many grouped lifeforms (Bai et al. 2004). Such groupings are based on the idea that ecologically-
432 similar species will have similar environmental responses through time, a valid assumption with-
433 out evidence to the contrary. At first glance our results may appear to support the grouping of
434 perennial grasses because their environmental responses were correlated. However, even though
435 environmental responses among the dominant species we studied were similar, they were dis-
436 similar enough to cause synchrony to be less than perfect (Fig. 2). The subtle differences among
437 ecologically-similar dominant species does impact species synchrony and, ultimately, ecosys-
438 tem stability. Ignoring such difference may, though not always, mask important dynamics that

439 underpin ecosystem functioning.

440 **Interspecific interactions had little impact on community synchrony**

441 We expected community synchrony of per capita growth rates to decrease when we removed
442 interspecific interactions (Loreau and de Mazancourt 2008). We found that community synchrony
443 was virtually indistinguishable between simulations with and without interspecific interactions
444 (Fig. 2). The lack of an effect of interspecific interactions on synchrony is in contrast to a large
445 body of theoretical work that predicts a strong role for competition in creating compensatory
446 dynamics (Tilman 1988) and a recent empirical analysis (Gross et al. 2014).

447 Our results do not contradict the idea that competition can lead to compensatory dynamics,
448 but they do highlight the fact that interspecific competition must be relatively strong to influence
449 species synchrony. The communities we analyzed are composed of species with very little niche
450 overlap (Chu and Adler 2015) and weak interspecific interactions (Tables S1 and S3-S17). Mech-
451 anistic consumer-resource models (Lehman and Tilman 2000) and phenomenological Lotka-
452 Volterra models (Lehman and Tilman 2000, Loreau and de Mazancourt 2013) both confirm that
453 the effect of competition on species synchrony diminishes as niche overlap decreases. In that
454 sense, our results are not surprising: interspecific interactions are weak, so of course removing
455 them does not affect synchrony.

456 Our conclusion that species interactions have little impact on synchrony only applies to
457 single trophic level communities. Species interactions almost certainly play a strong role in multi-
458 trophic communities where factors such as resource overlap (Vasseur and Fox 2007), dispersal
459 (Gouhier et al. 2010), and the strength of top-down control (Bauer et al. 2014) are all likely to
460 affect community synchrony.

CONCLUSIONS

462 Species-specific responses to temporally fluctuating environmental conditions is an important
463 mechanism underlying asynchronous population dynamics and, in turn, ecosystem stability
464 (Loreau and de Mazancourt 2013). When we removed environmental variation, we found that
465 synchrony decreased in four out of the five grassland communities we studied (Fig. 2). A tempt-
466 ing conclusion is that our study confirms that compensatory dynamics are rare in natural commu-
467 nities, and that ecologically-similar species will exhibit synchronous dynamics (e.g., Houlahan et
468 al. 2007). Such a conclusion misses an important subtlety. The perennial grasses we studied do
469 have similar responses to the environment (Table S2), which will tend to synchronize dynamics.
470 However, if community-wide synchrony **among dominant species** is less than 1, as it is in all
471 our focal communities, some degree of compensatory dynamics must be present (Loreau and de
472 Mazancourt 2008). Even ecologically-similar species, which are sometimes aggregated into to
473 functional groups, have environmental responses that are dissimilar enough to cause asynchrony.
474 Subtle differences among dominant species ultimately determine ecosystem stability and should
475 not be ignored.

ACKNOWLEDGEMENTS

477 This work was funded by the National Science Foundation through a Postdoctoral Research
478 Fellowship in Biology to ATT (DBI-1400370) and a CAREER award to PBA (DEB-1054040).
479 CdM and ML were supported by the TULIP Laboratory of Excellence (ANR-10-LABX-41).
480 We thank the original mappers of the permanent quadrats at each site and the digitizers in the
481 Adler lab, without whom this work would not have been possible. Compute, storage, and other
482 resources from the Division of Research Computing in the Office of Research and Graduate
483 Studies at Utah State University are gratefully acknowledged. We also thank several anonymous
484 reviewers who provided critical feedback that improved the manuscript.

485 **Tables**

486 Table 1: Site descriptions and focal species.

Site Name	Biome	Location (Lat, Lon)	Obs. Years	Species
New Mexico	Chihuahuan Desert	32.62° N, 106.67° W	1915-1950	<i>Bouteloua eriopoda</i> <i>Sporobolus flexuosus</i>
Arizona	Sonoran Desert	31°50' N, 110°53' W	1915-1933	<i>Bouteloua eriopoda</i> <i>Bouteloua rothrockii</i>
Kansas	Southern mixed prairie	38.8° N, 99.3° W	1932-1972	<i>Bouteloua curtipendula</i> <i>Bouteloua hirsuta</i> <i>Schizachyrium scoparium</i>
Montana	Northern mixed prairie	46°19' N, 105°48' W	1926-1957	<i>Bouteloua gracilis</i> <i>Hesperostipa comata</i> <i>Pascopyrum smithii</i> <i>Poa secunda</i>
Idaho	Sagebrush steppe	44.2° N, 112.1° W	1926-1957	<i>Artemisia tripartita</i> <i>Pseudoroegneria spicata</i> <i>Hesperostipa comata</i> <i>Poa secunda</i>

Table 2: Observed synchrony among species' per capita growth rates (ϕ_R), observed synchrony among species' percent cover (ϕ_C), the coefficient of variation of total community cover, and species richness for each community. Species richness values reflect the number of species analyzed from the community, not the actual richness.

Site	ϕ_R	ϕ_C	CV of Total Cover	Species richness
New Mexico	0.86	0.92	0.51	2
Arizona	0.89	0.80	0.47	2
Kansas	0.54	0.15	0.30	3
Montana	0.53	0.54	0.52	4
Idaho	0.36	0.18	0.19	4

487 **Figures**

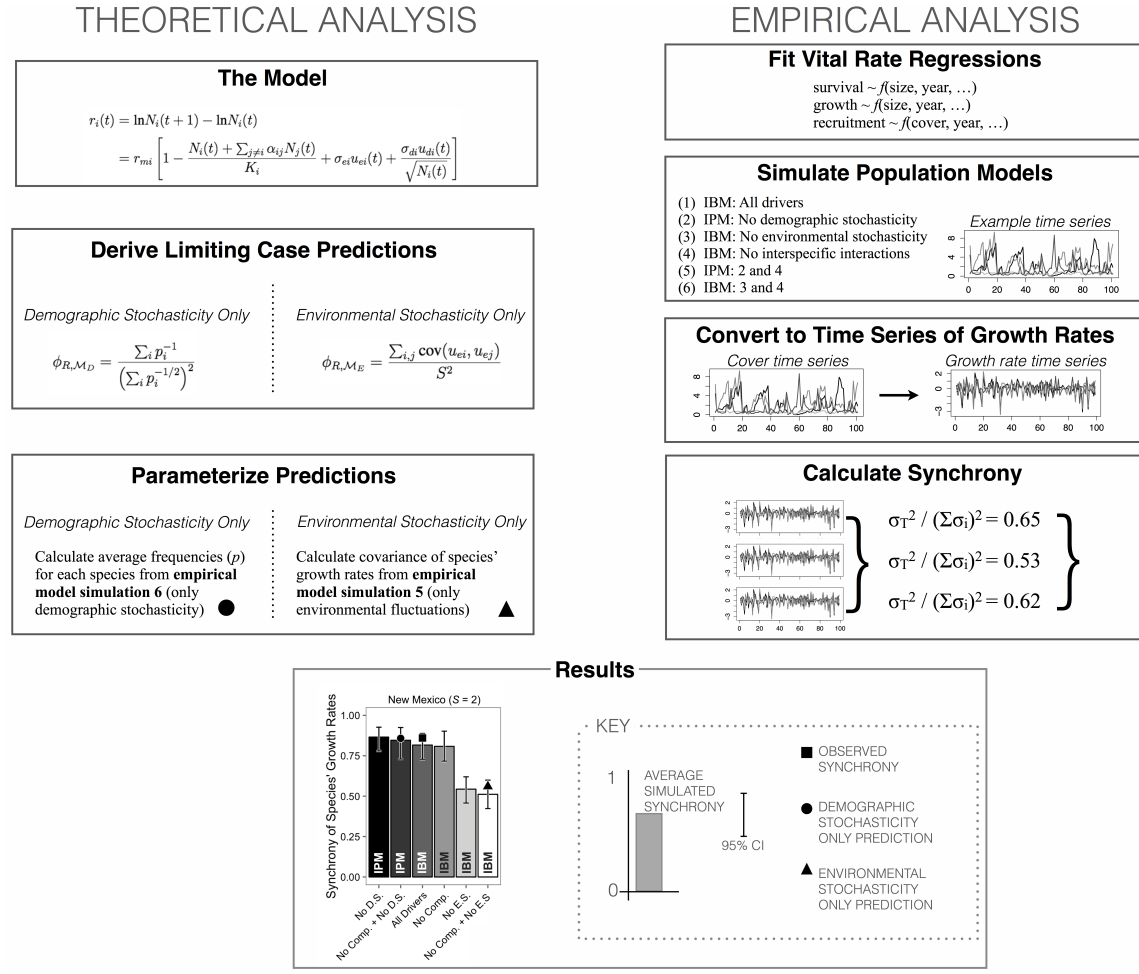


Figure 1: Diagram of our coupled theoretical-empirical approach.

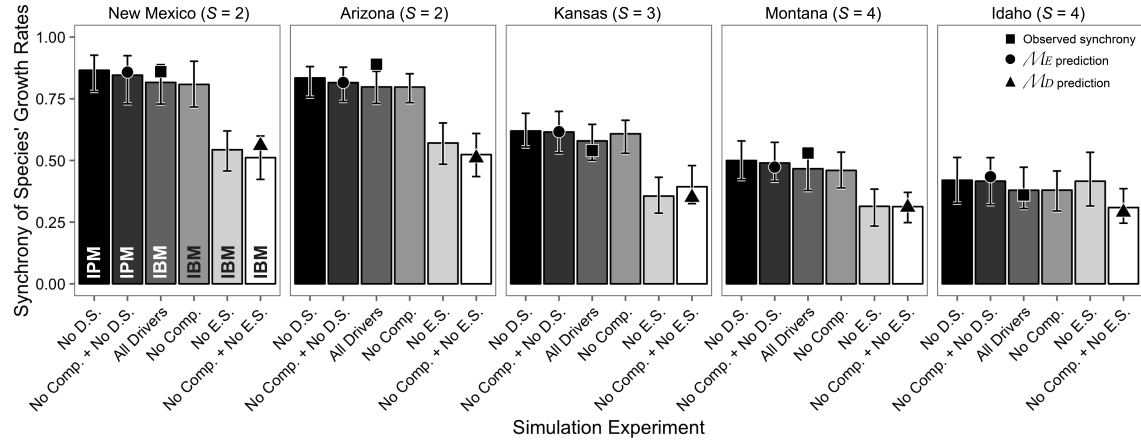


Figure 2: Community-wide species synchrony of per capita growth rates from model simulation experiments. Synchrony of species' growth rates for each study area are from simulation experiments with demographic stochasticity, environmental stochasticity, and interspecific interactions present (“All Drivers”), demographic stochasticity removed (“No D.S.”), environmental stochasticity removed (“No E.S.”), interspecific interactions removed (“No Comp.”), interspecific interactions and demographic stochasticity removed (“No Comp. + No D.S.”), and interspecific interactions and environmental stochasticity removed (“No Comp. + No E.S.”). Abbreviations within the bars for the New Mexico site indicate whether the IBM or IPM was used for a particular simulation. Error bars represent the 2.5% and 97.5% quantiles from model simulations. All IBM simulations shown in this figure were run on a 25 m^2 virtual landscape. Points show observed and predicted synchrony aligned with the model simulation that corresponds with each observation or analytical prediction.

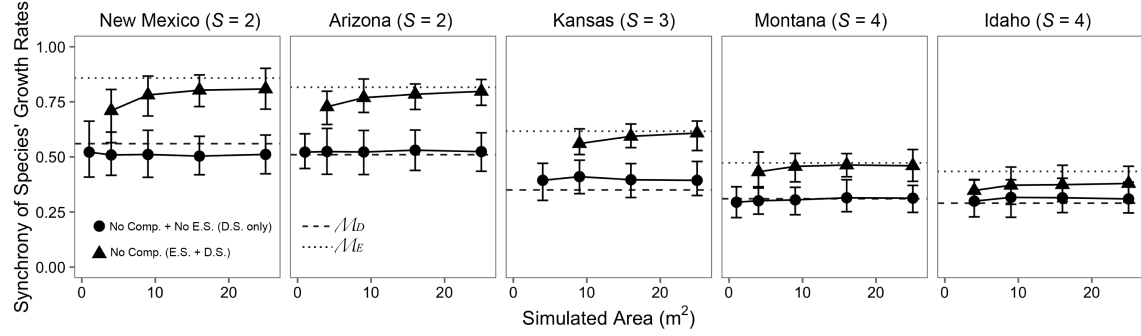


Figure 3: Synchrony of species' growth rates for each study area from IBM simulations across different landscape sizes when only demographic stochasticity is present (“No Comp. + No E.S. (D.S. Only)”) and when environmental stochasticity is also present (“No Comp. (D.S. + E.S.)”). The horizontal lines show the analytical predictions \mathcal{M}_D (dashed line) and \mathcal{M}_E (dotted line). The strength of demographic stochasticity decreases as landscape size increases because population sizes also increase. Theoretically, “No Comp. + No E.S. (D.S. Only)” simulations should remain constant across landscape size, whereas “No Comp. (D.S. + E.S.)” simulations should shift from the \mathcal{M}_D prediction to the \mathcal{M}_E prediction as landscape size, and thus population size, increases, but only if demographic stochasticity is strong enough to counteract environmental forcing. Error bars represent the 2.5% and 97.5% quantiles from model simulations.

488 **References**

- 489 Adler, P. B., S. P. Ellner, and J. M. Levine. 2010. Coexistence of perennial plants: An embarrass-
490 ment of niches. *Ecology Letters* 13:1019–1029.
- 491 Adler, P. B., W. R. Tyburczy, and W. K. Lauenroth. 2007. Long-term mapped quadrats from
492 Kansas prairie: demographic information for herbaceous plants. *Ecology* 88:2673.
- 493 Anderson, J., M. P. McClaran, and P. B. Adler. 2012. Cover and density of semi-desert grassland
494 plants in permanent quadrats mapped from 1915 to 1947. *Ecology* 93:1492–1492.
- 495 Anderson, J., L. Vermeire, and P. B. Adler. 2011. Fourteen years of mapped, permanent quadrats
496 in a northern mixed prairie, USA. *Ecology* 92:1703.
- 497 Bai, Y., X. Han, J. Wu, Z. Chen, and L. Li. 2004. Ecosystem stability and compensatory effects
498 in the Inner Mongolia grassland. *Nature* 431:181–184.
- 499 Bauer, B., M. Vos, T. Klauschies, and U. Gaedke. 2014. Diversity, Functional Similarity, and Top-
500 Down Control Drive Synchronization and the Reliability of Ecosystem Function. *The American
501 Naturalist* 183:394–409.
- 502 Cardinale, B. J., J. E. Duffy, A. Gonzalez, D. U. Hooper, C. Perrings, P. Venail, A. Narwani, G.
503 M. Mace, D. Tilman, D. A. Wardle, A. P. Kinzig, G. C. Daily, M. Loreau, and J. B. Grace. 2012.
504 Biodiversity loss and its impact on humanity. *Nature* 489:59–67.
- 505 Chu, C., and P. B. Adler. 2015. Large niche differences emerge at the recruitment stage to stabi-
506 lize grassland coexistence. *Ecological Monographs* 85:373–392.
- 507 de Mazancourt, C., F. Isbell, A. Larocque, F. Berendse, E. De Luca, J. B. Grace, B. Haegeman, H.
508 Wayne Polley, C. Roscher, B. Schmid, D. Tilman, J. van Ruijven, A. Weigelt, B. J. Wilsey, and
509 M. Loreau. 2013. Predicting ecosystem stability from community composition and biodiversity.
510 *Ecology Letters* 16:617–625.
- 511 Dornelas, M., N. J. Gotelli, B. McGill, H. Shimadzu, F. Moyes, C. Sievers, and A. E. Magur-
512 ran. 2014. Assemblage time series reveal biodiversity change but not systematic loss. *Science*
513 344:296–9.
- 514 Gonzalez, A., and M. Loreau. 2009. The Causes and Consequences of Compensatory Dynamics
515 in Ecological Communities. *Annual Review of Ecology, Evolution, and Systematics* 40:393–414.
- 516 Gouhier, T. C., and F. Guichard. 2014. Synchrony: quantifying variability in space and time.
517 *Methods in Ecology and Evolution* 5:524–533.
- 518 Gouhier, T. C., F. Guichard, and A. Gonzalez. 2010. Synchrony and Stability of Food Webs in
519 Metacommunities. *The American Naturalist* 175:E16–E34.
- 520 Grman, E., J. A. Lau, D. R. Schoolmaster, and K. L. Gross. 2010. Mechanisms contributing to
521 stability in ecosystem function depend on the environmental context. *Ecology Letters* 13:1400–
522 1410.
- 523 Gross, K., B. J. Cardinale, J. W. Fox, A. Gonzalez, M. Loreau, H. W. Polley, P. B. Reich, and
524 J. van Ruijven. 2014. Species richness and the temporal stability of biomass production: a new
525 analysis of recent biodiversity experiments. *The American naturalist* 183:1–12.

- 526 Hautier, Y., E. W. Seabloom, E. T. Borer, P. B. Adler, W. S. Harpole, H. Hillebrand, E. M. Lind,
527 A. S. MacDougall, C. J. Stevens, J. D. Bakker, Y. M. Buckley, C. Chu, S. L. Collins, P. Daleo, E.
528 I. Damschen, K. F. Davies, P. a Fay, J. Firn, D. S. Gruner, V. L. Jin, J. a Klein, J. M. H. Knops, K.
529 J. La Pierre, W. Li, R. L. McCulley, B. a Melbourne, J. L. Moore, L. R. O'Halloran, S. M. Prober,
530 A. C. Risch, M. Sankaran, M. Schuetz, and A. Hector. 2014. Eutrophication weakens stabilizing
531 effects of diversity in natural grasslands. *Nature* 508:521–5.
- 532 Hector, A., Y. Hautier, P. Saner, L. Wacker, R. Bagchi, J. Joshi, M. Scherer-Lorenzen, E. M.
533 Spehn, E. Bazeley-White, M. Weilenmann, M. C. Caldeira, P. G. Dimitrakopoulos, J. a. Finn,
534 K. Huss-Danell, A. Jumpponen, and M. Loreau. 2010. General stabilizing effects of plant di-
535 versity on grassland productivity through population asynchrony and overyielding. *Ecology*
536 91:2213–2220.
- 537 Hooper, D., F. Chapin III, and J. Ewel. 2005. Effects of biodiversity on ecosystem functioning: a
538 consensus of current knowledge. *Ecological Monographs* 75:3–35.
- 539 Houlahan, J. E., D. J. Currie, K. Cottenie, G. S. Cumming, S. K. M. Ernest, C. S. Findlay, S. D.
540 Fuhlendorf, U. Gaedke, P. Legendre, J. J. Magnuson, B. H. McArdle, E. H. Muldavin, D. Noble,
541 R. Russell, R. D. Stevens, T. J. Willis, I. P. Woiwod, and S. M. Wondzell. 2007. Compensatory
542 dynamics are rare in natural ecological communities. *Proceedings of the National Academy of
543 Sciences of the United States of America* 104:3273–3277.
- 544 Isbell, F. I., H. W. Polley, and B. J. Wilsey. 2009. Biodiversity, productivity and the temporal
545 stability of productivity: Patterns and processes. *Ecology Letters* 12:443–451.
- 546 Lande, R., S. Engen, and B.-E. Saether. 2003. Stochastic population dynamics in ecology and
547 conservation.
- 548 Lehman, C. L., and D. Tilman. 2000. Biodiversity, Stability, and Productivity in Competitive
549 Communities. *The American Naturalist* 156:534–552.
- 550 Loreau, M., and C. de Mazancourt. 2008. Species synchrony and its drivers: neutral and nonneu-
551 tral community dynamics in fluctuating environments. *The American Naturalist* 172:E48–E66.
- 552 Loreau, M., and C. de Mazancourt. 2013. Biodiversity and ecosystem stability: A synthesis of
553 underlying mechanisms. *Ecology Letters* 16:106–115.
- 554 Loreau, M., and a Hector. 2001. Partitioning selection and complementarity in biodiversity exper-
555 iments. *Nature* 412:72–6.
- 556 Loreau, M., S. Naeem, P. Inchausti, J. Bengtsson, J. P. Grime, A. Hector, D. U. Hooper, M. A.
557 Huston, D. Raffaelli, B. Schmid, D. Tilman, and D. A. Wardle. 2001. Biodiversity and ecosystem
558 functioning: current knowledge and future challenges. *Science* 294:804–808.
- 559 Mutshinda, C. M., R. B. O'Hara, and I. P. Woiwod. 2009. What drives community dynamics?
560 *Proceedings of the Royal Society B: Biological Sciences* 276:2923–2929.
- 561 Plummer, M. 2003. JAGS: A Program for Analysis of Bayesian Graphical Models Using Gibbs
562 Sampling. Pages 20–22 in *Proceedings of the 3rd international workshop on distributed statistical
563 computing (dSC 2003)*. march.
- 564 Plummer, M. 2014. *rjags*: Bayesian graphical models using MCMC.

- 565 R Core Team. 2013. R: A language and environment for statistical computing.
- 566 Ranta, E., V. Kaitala, M. S. Fowler, J. Laakso, L. Ruokolainen, and R. O'Hara. 2008. Detecting
567 compensatory dynamics in competitive communities under environmental forcing. *Oikos*
568 117:1907–1911.
- 569 Rockstrom, J., J. Rockstrom, W. Steffen, W. Steffen, K. Noone, K. Noone, A. Persson, A. Pers-
570 son, F. S. Chapin, F. S. Chapin, E. F. Lambin, E. F. Lambin, T. M. Lenton, T. M. Lenton, M.
571 Scheffer, M. Scheffer, C. Folke, C. Folke, H. J. Schellnhuber, H. J. Schellnhuber, B. Nykvist, B.
572 Nykvist, C. A. de Wit, C. A. de Wit, T. Hughes, T. Hughes, S. van der Leeuw, S. van der Leeuw,
573 H. Rodhe, H. Rodhe, S. Sorlin, S. Sorlin, P. K. Snyder, P. K. Snyder, R. Costanza, R. Costanza,
574 U. Svedin, U. Svedin, M. Falkenmark, M. Falkenmark, L. Karlberg, L. Karlberg, R. W. Corell,
575 R. W. Corell, V. J. Fabry, V. J. Fabry, J. Hansen, J. Hansen, B. Walker, B. Walker, D. Liverman,
576 D. Liverman, K. Richardson, K. Richardson, P. Crutzen, P. Crutzen, J. A. Foley, and J. A. Foley.
577 2009. A safe operating space for humanity. *Nature* 461:472–475.
- 578 Rue, H., S. Martino, and N. Chopin. 2009. Approximate Bayesian Inference for Latent Gaussian
579 Models Using Integrated Nested Laplace Approximations. *Journal of the Royal Statistical
580 Society, Series B* 71:319–392.
- 581 Rue, H., S. Martino, F. Lindgren, D. Simpson, A. Riebler, and E. Teixeira. 2014. INLA: Func-
582 tions which allow to perform full Bayesian analysis of latent Gaussian models using Integrated
583 Nested Laplace Approximation.
- 584 Sasaki, T., and W. K. Lauenroth. 2011. Dominant species, rather than diversity, regulates tempo-
585 ral stability of plant communities. *Oecologia* 166:761–768.
- 586 Smith, M. D., and A. K. Knapp. 2003. Dominant species maintain ecosystem function with non-
587 random species loss. *Ecology Letters* 6:509–517.
- 588 Taylor, L. R. 1961. Aggregation, Variance and the Mean. *Nature* 189:732–735.
- 589 Thibaut, L. M., S. R. Connolly, and H. P. A. Sweatman. 2012. Diversity and stability of herbivo-
590 rous fishes on coral reefs. *Ecology* 93:891–901.
- 591 Tilman, D. 1988. Plant strategies and the dynamics and structure of plant communities. *Plant
592 strategies and the dynamics and structure of plant communities*.:360 pp.
- 593 Tilman, D., P. B. Reich, and J. M. H. Knops. 2006. Biodiversity and ecosystem stability in a
594 decade-long grassland experiment. *Nature* 441:629–632.
- 595 Tilman, D., P. B. Reich, J. Knops, D. Wedin, T. Mielke, and C. Lehman. 2001. Diversity and
596 productivity in a long-term grassland experiment. *Science* 294:843–845.
- 597 Vasseur, D. A., and J. W. Fox. 2007. Environmental fluctuations can stabilize food web dynamics
598 by increasing synchrony. *Ecology Letters* 10:1066–1074.
- 599 Vellend, M., L. Baeten, I. H. Myers-Smith, S. C. Elmendorf, R. Beauséjour, C. D. Brown, P.
600 De Frenne, K. Verheyen, and S. Wipf. 2013. Global meta-analysis reveals no net change in
601 local-scale plant biodiversity over time. *Proceedings of the National Academy of Sciences of
602 the United States of America* 110:19456–9.
- 603 Venail, P. A., M. A. Alexandrou, T. H. Oakley, and B. J. Cardinale. 2013. Shared ancestry in-
604 fluences community stability by altering competitive interactions: evidence from a laboratory

- 605 microcosm experiment using freshwater green algae. *Proceedings of the Royal Society of Lon-*
606 *don B: Biological Sciences* 280.
- 607 Vitousek, P. M., H. a Mooney, J. Lubchenco, and J. M. Melillo. 1997. Human Domination of
608 Earth's Ecosystems. *Science* 277:494–499.
- 609 Wang, S., and M. Loreau. 2014. Ecosystem stability in space: α , β and γ variability. *Ecology*
610 Letters 17:891–901.
- 611 Wang, S., and M. Loreau. 2016. Biodiversity and ecosystem stability across scales in metacom-
612 munities. *Ecology Letters*.
- 613 Yachi, S., and M. Loreau. 1999. Biodiversity and ecosystem productivity in a fluctuating environ-
614 ment: the insurance hypothesis. *Proceedings of the National Academy of Sciences of the United*
615 *States of America* 96:1463–1468.
- 616 Zachmann, L., C. Moffet, and P. Adler. 2010. Mapped quadrats in sagebrush steppe: long-term
617 data for analyzing demographic rates and plant–plant interactions. *Ecology* 91:3427.